

Model 1

Model 2

Model 3

Model 4

Model 5

Model 6

Why cold slabs stagnate in the transition zone

Scott D. King^{1,2}, Daniel J. Frost², and David C. Rubie²

¹*Department of Geosciences, Virginia Tech, Blacksburg, Virginia 24061, USA*

²*Bayerisches Geoinstitut, Universität Bayreuth, D-95440 Bayreuth, Germany*

Supplemental Material

This document contains supplemental material documenting the equilibrium formulation for the pyroxene-majorite transformation implemented in the convection code, a technical discussion of the transition temperature between equilibrium and non-equilibrium phase transformation based on the slow diffusion laboratory results of van Mierlo et al. (2013) and documentation of the composite rheology used in the convection modeling. We also include the phase diagram for the olivine-wadsleyite-ringwoodite transformation adapted from Frost (2008).

Equilibrium Pyroxene-Majorite Transformation

For the pyroxene to garnet-majorite transformation, we use a parameterized equilibrium thermodynamic formulation that assumes a 50:50 mixture of pyrope and pyroxene as a starting point using parameters from Stixrude and Lithgow-Bertelloni (2011). The formulation is as follows. For the Gibbs free energy, G , we have

$$G = 126771 + 3.07T - 7141P \quad (1)$$

where P and T are pressure (in GPa) and temperature (in K). The mole fraction of majorite, Y , is then given by

$$Y = \exp\left(-\frac{G}{8.314T}\right) \quad (2)$$

and finally density (in kg/m³) is given by

$$\rho_{px_gt} = \frac{40000}{0.5a + (0.5 - Y)b + Yc} \quad (3)$$

where

$$a = 11.611 - 0.0533P \quad (4)$$

$$b = 12.651 - 0.0724P \quad (5)$$

$$c = 11.723 - 0.0568P. \quad (6)$$

This is shown in Fig. S2 where we have scaled the density by $\rho\alpha\Delta T$. To assess the effect of slow diffusion of majoritic garnet on the phase transformation at low temperatures, we applied a hyperbolic tangent function to Equation (3) as follows

$$\rho_{px_gt} = \frac{40000}{0.5a + (0.5 - Y)b + Yc} - \tanh\left(\frac{T - T_{trans}}{100} + 1\right) \quad (7)$$

where T_{trans} is the transition temperature below which slow-diffusion occurs.

Transition Temperature

In order to model the effects of pyroxene metastability, we use a critical transition temperature. Below this temperature, pyroxene is considered to remain metastable up to a pressure of 18 GPa whereas above the transition temperature it is considered to transform rapidly to majoritic garnet. For comparison, in the case of the olivine-spinel transformation, the transition temperature has been estimated to be 900-950 K (Rubie and

Ross, 1994). For the majorite-forming reaction, relevant diffusion coefficients can be determined as a function of temperature from the activation energy and the pre-exponential factor determined by van Mierlo et al. (2013). Diffusion distances are then calculated assuming a timescale of 3 My for the descent of a slab through the transition zone and are compared with the expected grain size of 5-10 mm – which gives the diffusion distance required for complete transformation. Diffusion distances thus calculated are 60 μm at 1000 K, 0.2 mm at 1200 K, 0.5 mm at 1300 K and 1.2 mm at 1400 K. Based on these results, we assume for most calculations that the transition is 1200 K because this results in an extent of transformation that is finite but small compared with the expected grain size. However, this value is on the conservative side and a value of 1300 K would also be reasonable. Using the latter would produce even stronger buoyancy/stagnation effects than are documented for 1200 K.

Composite Rheology

Following Hirth and Kohlstedt (2003) we define the effective viscosity as,

$$\eta = \left(\frac{1}{A}\right)^{\frac{1}{n}} (d)^{\frac{p}{n}} fH_2O^{\frac{r}{n}} \exp(-\alpha\phi) \dot{\varepsilon}^{\left(\frac{1}{n}-1\right)} \exp\left[\frac{(E^* + PV^*)}{nRT}\right] \quad (8)$$

where A is a pre-exponential factor, n is the stress exponent, d is the grain-size, p is the grain-size exponent, fH_2O is the water fugacity, r is the water fugacity exponent, ϕ is the melt fraction, α is a constant, $\dot{\varepsilon}$ is the strain-rate, E^* is the activation energy, V^* is the activation volume, R is the gas constant. This form of the equation assumes that the stress is given in MPa, grain size in μm and fH_2O or C_{OH} in H/10⁶Si. We do not consider melt and thus $\phi=0$.

For diffusion creep, also called a linear rheology or Newtonian rheology, the stress exponent is one (i.e., $n=1$) and thus, the strain-rate-dependent term is always 1.0. The diffusion creep mechanism is a function of grain size (Hirth and Kohlstedt, 2003). Following Billen and Hirth (2007) we modify the activation volume for the lower mantle to be $1.5 \times 10^{-6} \text{ m}^3/\text{mole}$ and modify the pre-exponential term so that there is a factor of 30 increase in lower mantle viscosity.

Dislocation creep, or power-law or non-Newtonian rheology is given by the same equation above (eqn 8), except that now the stress exponent is greater than 1 (i.e., $n=3.5$) and is independent of grain size ($p=0$). Following Billen and Hirth (2007) we define the composite rheology, η_{comp} , as

$$\eta_{comp} = \frac{1.0}{\frac{1.0}{\eta_{dif}} + \frac{1.0}{\eta_{disl}}}, \quad (9)$$

where η_{dif} is diffusion creep rheology and η_{disl} is dislocation creep rheology. This weighted average is only used in the upper 400 km, as below this depth, the mantle is seismically isotropic and this suggests that diffusion creep dominates (King, 2007). For numerical stability we truncate the viscosity so that the maximum viscosity is no more than 10^5 times the background viscosity. This has been shown to be large enough viscosity contrast that truncation of larger viscosities does not affect the resulting flow (King, 2009).

References

- Akaogi, M., and Ito, E., 1993, Heat capacity of MgSiO₄ perovskite: Geophysical Research Letters, v. 20, p. 105–108.
- Bina, C. R., and Helffich, G., 1994, Phase transition Clapeyron slopes and transition zone seismic discontinuity topography: Journal of Geophysical Research, v. 99, p. 15,853–15,860.
- Billen, M. I., 2008, Modeling the dynamics of subducting slabs: Annual Reviews of Earth and Planetary Science, v 36, p. 325–356.
- Billen, M. I., and Hirth, G., 2007, Rheologic controls on slab dynamics: Geochemistry Geophysics Geosystems, v. 8, Q08012, doi:10.1029/2007GC001597.
- Fei, Y., Van Orman, J. Li, J., van Westrenen, W., Sanloup, C., et al., 2004, Experimentally determined postspinel transformation boundary in Mg₂SiO₄ using MgO as an internal pressure standard and its geophysical implications: Journal of Geophysical Research, v. 109, B02305.
- Frost, D.J., 2008, The upper mantle and transition zone: Elements, v. 4, p. 171–176, doi:10.2113/GSELEMENTS.4.3.171.
- Hirth, G., and Kohlstedt, D., 2003, Rheology of the upper mantle and the mantle wedge: A view from the experimentalists, in Inside the Subduction Factory, Geophys. Monogr. Ser. 138 edited by J. Eiler, pp. 83–105 AGU, Washington, D. C.
- Irfune, T., Nishiyama, N., Kuroda, K., Inoue, T., Isshiki, T, M., et al., 1998, The postspinel phase boundary in Mg₂ SiO₄ determined by in situ X-ray diffraction: Science, v. 279, p. 1698–1700.

- Ito, E., and Takahashi, E., 1989, Postspinel transformations in the system Mg₂SiO₄-Fe₂SiO₄ and some geophysical implications: *Journal of Geophysical Research*, v. 94, p. 10,637–10,646.
- Katsura, T., Yamada, H., Shinmei, T., Kubo, A., Ono, S., et al., 2003, Post-spinel transition in Mg₂SiO₄ determined by high P-T in situ X-ray diffractometry: *Physics of the Earth and Planetary Interiors*, v. 136, p. 11–24.
- King, S.D., 2009, On topography and geoid from 2-D stagnant lid convection calculations: *Geochemistry, Geophysics, Geosystems*, v. 10, Q03002, doi:10.1029/2008GC002250.
- King, S.D., 2007, Mantle downwellings and the fate of subducting slabs: Constraints from seismology, geoid, topography, geochemistry, and petrology. in *Treatise on Geophysics, Volume 7, Mantle Dynamics*, pp. 325–370.
- Litasov, K.D., Ohtani, E., Sano, A., and Suzuki, A., 2005a, Wet subduction versus cold subduction: *Geophysical Research Letters*, v.32, L13312.
- Litasov, K.D., Ohtani, E., Sano, A., Suzuki, A., and Funakoshi K., 2005b, *Earth and Planetary Science Letters*, v. 238, p. 311–328.
- Rubie, D.C., and Ross, C.R., 1994, II, Kinetics of the olivine-spinel transformation in subducting lithosphere: Experimental constraints and implications for deep slab processes: *Physics of the Earth and Planetary Interiors*, v. 86, p. 223–241.
- Stixrude, L., and Lithgow-Bertelloni, C., 2011, Thermodynamics of mantle minerals – II. Phase equilibria: *Geophysical Journal International*, v. 184, p. 1180–1213.

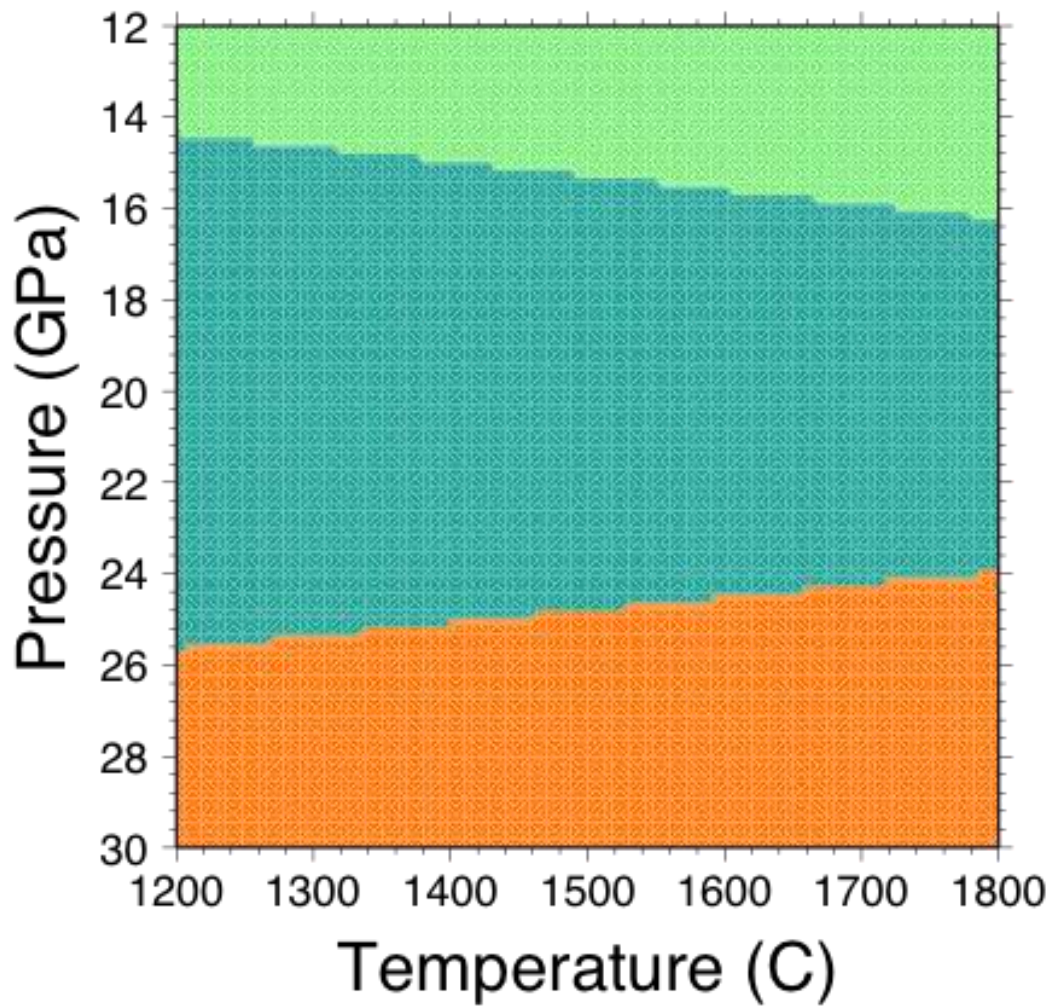


Figure S1: Phase diagram for the olivine mantle component as implemented in our subduction calculations. Light green is olivine, dark green is the ‘transition zone’ (wadsleyite and ringwoodite) and orange is the bridgmanite plus ferropericlase component.

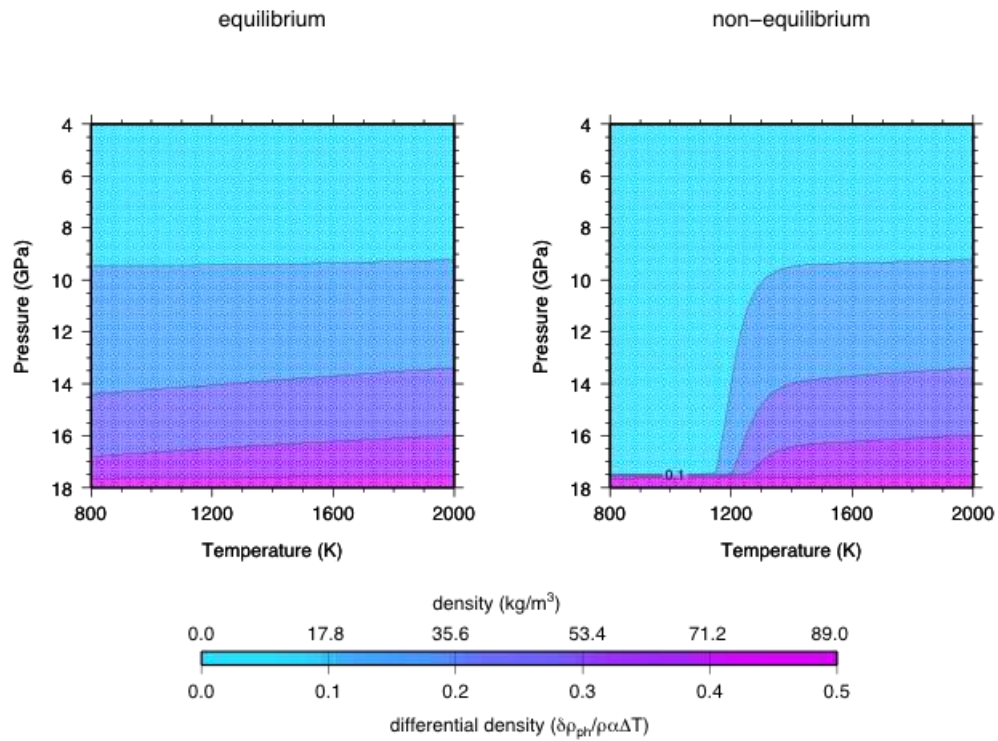


Figure S2: Relative density of the pyroxene-garnet phase transformation scaled by $\rho\alpha\Delta T$ using equations (1)-(6). The non-equilibrium version is created by applying a hyperbolic tangent function to equation (7) as described in the text.

Model Parameters	Earth Value
reference density	$3.3 \times 10^3 \text{ kg/m}^3$
coefficient of thermal expansion	$2.0 \times 10^{-5} \text{ K}^{-1}$
surface gravity	10 m/s^2
surface temperature	273 K
convective temperature drop	1875 K
depth of the mantle	$2.890 \times 10^6 \text{ m}$
thermal diffusivity	$10^{-6} \text{ m}^2/\text{s}$
reference viscosity	10^{20} Pa s
Rayleigh number	3.0×10^8

Table 1: Model Parameters

Clapeyron Slope MPa/K	Reference
-2.8	Ito and Takahashi (1989)
-3.0	Akaogi and Ito (1993)
-2.9	Irifune et al. (1998)
-2.0	Bina and Helffich (1994)
-0.4 to -2.0	Katsura et al. (2003)
-1.3	Fei et al. (2004)
-0.5 to -0.8 (dry)	Litasov et al. (2005a)
-2.0 (hydrus)	Litasov et al. (2005b)

Table 2: Published values of the Clapeyron Slope for the ringwoodite to perovskite plus ferropericlase transformiaon.

Study	A	n	p	E^* (kJ/mole)	V^* $10^{-6} \text{ m}^3/\text{mole}$
HK03 dry	1.5×10^9	1	3	375 ± 50	2-10
HK03 wet	2.5×10^7	1	3	375 ± 50	0-20
BH07	1.0	1	3	335	4
this study	1.0	1	3	335	4

Table 3: Diffusion Creep Model Parameters

Study	A	n	p	E^* (kJ/mole)	V^* $10^{-6} \text{ m}^3/\text{mole}$
HK03 dry	1.1×10^5	3.5 ± 0.3	0	520 ± 40	0-20
HK03 wet	1.6×10^3	3.5 ± 0.3	0	480 ± 40	22 ± 11
BH07	90×10^{21}	3.5	0	480	11
this study	90×10^{21}	3.5	0	480	11

Table 4: Dislocation Creep Model Parameters